Charge Distribution in a Kondo-Correlated Quantum Dot

D. Sprinzak, Yang Ji, M. Heiblum, D. Mahalu, and Hadas Shtrikman
Braun Center for Submicron Research, Department of Condensed Matter Physics, Weizmann Institute of Science, Rehovot 76100, Israel
(Received 19 October 2001; published 12 April 2002)

We report on direct measurement of charge and its distribution in a Kondo correlated quantum dot (QD). A noninvasive potential-sensitive detector, in proximity with a QD, reveals that, although the conductance of the QD is significantly enhanced as it enters the Kondo regime, the average charge remains unaffected. This demonstrates the separation between spin and charge degrees of freedom. We find, however, under certain conditions, an abrupt redistribution of charge in the QD, taking place with an onset of Kondo correlation. This suggests a correlation between the spin and charge degrees of freedom.

DOI: 10.1103/PhysRevLett.88.176805 PACS numbers: 73.23.Hk, 72.15.Qm, 75.20.Hr

The Kondo effect is a celebrated many-body phenomena in solid-state physics [1]. It leads to an anomalous behavior of the conductance in metals doped lightly with magnetic impurities. The effect results from a many-body interaction between a singly occupied spin-degenerate level in the magnetic impurity and the electrons in the reservoir. Recent proposals [2], and subsequent observation of the effect [3] in a mesoscopic quantum dot (QD) [4], which, when occupied by an odd number of electrons, plays the role of the magnetic impurity, allowed systematic studies of the effect by varying many of the system's parameters at will. The many-body interaction between a singly occupied spin-degenerate level in the QD and electrons in nearby reservoirs leads to spin reconfiguration in the reservoirs without affecting the charge distribution anywhere. In order to experimentally check that indeed charge configuration is not affected by the onset of Kondo correlations, we performed a direct, noninvasive, measurement of the charge distribution within a QD. A quantum point contact (QPC), located in close proximity to the QD, serves as a potential-sensitive, and hence charge-sensitive, detector [5]. The detector reveals that with the onset of Kondo correlation, the total, time averaged, charge in the dot remains indeed unaffected. However, with the application of a magnetic field the onset of the Kondo correlation is accompanied with an abrupt reconfiguration of the charge in the QD, without changing the total charge in it. Moreover, when the Kondo correlation diminishes, say, via pinching off the dot or increasing the temperature, and the QD enters the Coulomb blockade (CB) regime, such charge reconfiguration is not observed any more.

The device was fabricated in a GaAs heterostructure containing two dimensional electron gas with an areal electron density $n = 3.1 \times 10^{11}$ cm^{-2} and mobility $\mu = 5 \times 10^5$ cm^2 V^{-1} s^{-1} at $T = 4.2$ K. It [Fig. 1(a)] consists of a small QD, 170 nm in diameter, and an electrically separated QPC 200 nm away. The QPC serves as a potential detector [5]. Gate voltages V_{g1} and V_{g2} control the coupling of electrons in the QD to the source ($S_{\rm QD}$) and drain ($D_{\rm QD}$) reservoirs. As coupling strength increases, spin correlation forms between the QD and its leads, provided that the temperature is lower than the Kondo temperature $T_{\rm K}$. Consequently, for a QD with a nonzero net spin, the valley conductance increases—ideally reaching $2e^2/h$ at $T = 0$ (unitary limit). The induced potential in the QPC detector via the QD, $\phi_{\rm QPC}$, strongly affects its conductance [tuned to $G_{\rm QPC} \sim 0.5(2e^2/h)$ for highest sensitivity]. This potential depends linearly on the QD potential, $\phi_{\rm QD}$, which in turn depends on the net charge and its distribution in the QD, $\phi_{\rm QPC} = \phi_{\rm QD}\frac{C_{\rm QPC\text{-}QD}}{C_{\rm QPC}}$, with $C_{\rm QPC}$ the self-capacitance of the QPC and $C_{\rm QPC\text{-}QD}$ the mutual capacitance between QD and QPC. A small current (~40 nA) is driven across the QPC without a significant backaction on the QD (the Kondo enhanced conductance remains unaffected).

In the CB regime we expect $\phi_{\rm QD}$ to increase as the plunger gate voltage V_P increases, reaching $e/C_{\rm QD} + \Delta/e$, with $C_{\rm QD}$ the dot's capacitance and Δ the QD single particle level spacing in the QD. Another electron can now enter the QD and screen the positive potential induced by V_P. Hence, the QD potential and, consequently, the conductance of the QPC detector follow a sawtoothlike behavior. This ideal behavior is smeared either by the finite temperature of the electrons in the leads or by the finite energy width of the quantized levels in the QD, Γ [Fig. 1(b), center]. Weak features in $\phi_{\rm QPC}$ are better resolved by directly measuring the differential quantity $dI_{\rm QPC}/dV_P$, which shows a pronounced dip instead of a sawtoothlike behavior [Fig. 1(b), bottom]. A small ac modulation (1 mV) is added to V_P and the modulation of $I_{\rm QPC}$ is measured. A useful property of the QPC detector is shown in Fig. 1(c). As V_P gets more negative, the conductance peaks of the QD weaken and eventually cannot be resolved. This is due to inadvertent electrostatic coupling between plunger gate and other gates of the QD. Nevertheless, the dips in the detector's signal persist further until $V_P \sim -870$ mV, suggesting that the QD is depleted of electrons beyond this voltage. This allows an exact counting of the electrons in the QD.

We focus now on the characteristic double peak in the conductance, in the Kondo correlated regime, with nine electrons in the QD [Fig. 1(c)]. The detector signal in Fig. 2, at different temperatures and different

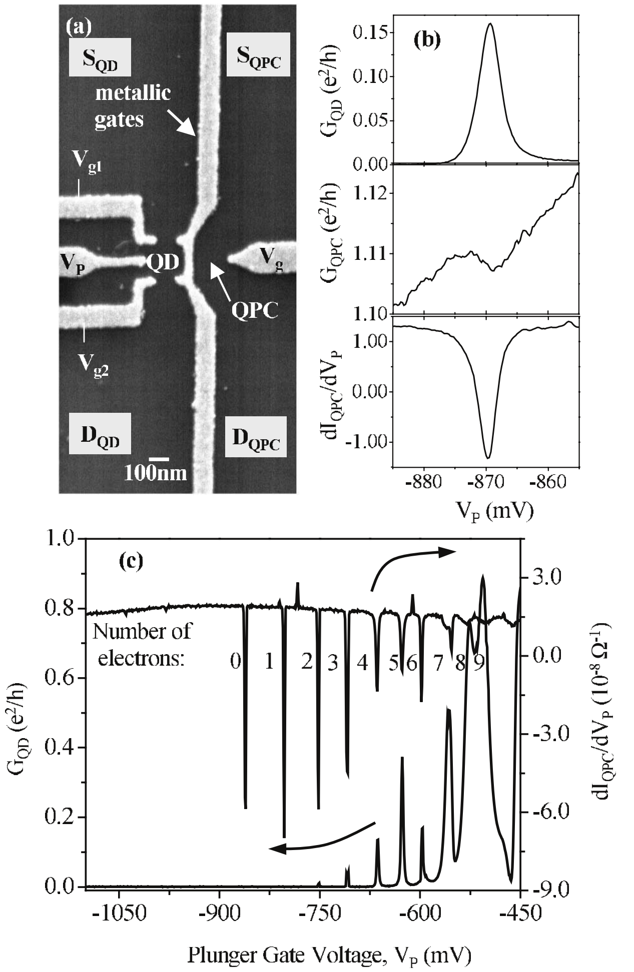

FIG. 1. (a) Scanning electron microscopy picture of the sample. (b) Top: a typical CB conductance peak of the QD. Middle: A typical measurement of the QPC detector. Bottom: a differential measurement of the detector signal. (c) Typical measurement of the QD conductance (bottom curve) and the detector signal (top curve) as a function of V_P. The number of electrons in each CB regime is shown in the figure. The double peak corresponds to nine electrons in the QD at the Kondo regime. Note that all data shown in the following figures were measured at similar but slightly different device configurations.

source-drain biases, shows that the potential evolution and the average charge in the QD do not change significantly when Kondo correlation is established. Hence, the enhancement in valley conductance results from a larger number of electrons traversing the QD, each dwelling there a shorter time. A short dwell time is expected due to the virtual nature of the cotunneling process [6]. This result shows that spin correlation is established without affecting the average charge distribution, namely, a separation of spin and charge degrees of freedom [7].

A careful look at the detector's signal, Fig. 1(c), reveals at least one sharp dip overlapping the broader, main dip, between seven and eight electrons in the QD. The emergence of such dips and their correlation with QD conductance becomes clearer in 2D color plots as function of V_P and magnetic field, B, applied normal to the plane [Fig. 3(a)]. The main features are horizontal yellow/blue lines, representing CB peaks and corresponding detector dips. Thus, electron filling is insensitive to the magnetic field in the scanned range. The prominent sharp dips initially overlap the broader dips, depart from them at higher magnetic fields, and curve upwards to cross subsequent broader dips. In exact coincidence with the detector dips a 2D plot of the conductance exhibits distinct boundaries separating regions of high (red/yellow) and low (blue) conductance. The regions of high and low conductance are identified as Kondo enhanced and CB valleys, respectively [8,9]. The sharp dips in the detector signal reflect abrupt changes in the QD potential, which must result from abrupt rearrangement of the charge in the QD (while the total charge is constant) [10]. The coincidence between the detector's dips and the onset of Kondo correlation surprisingly correlates charge reconfiguration and the Kondo effect.

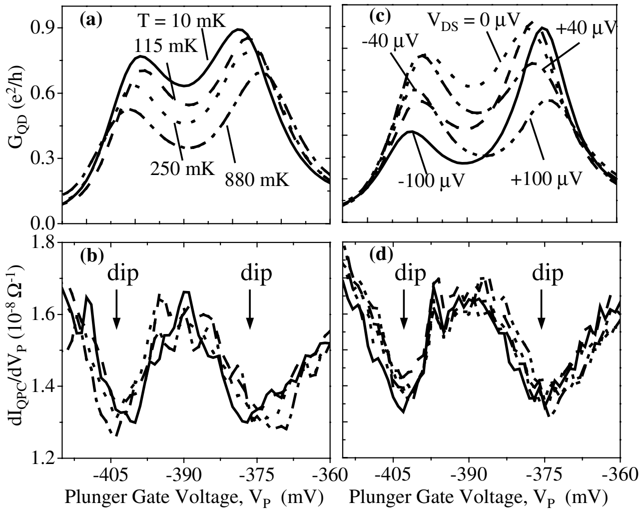

FIG. 2. (a) Conductance of the QD as a function of V_P at different temperatures (V_P is scanned over the region of V_P where 9 ± 1 electrons are in the QD. (b) Detector signal measured simultaneously with QD conductance in (a). (c) and (d) Conductance of the QD and detector signal as a function of V_P, for different drain-source bias on the QD, V_{DS}.

Pinching off the QD, by applying negative voltage to gates g_1 and g_2 or to the plunger gate, confines the electrons to the inner part of the QD, decoupling them from the reservoirs and quenching the Kondo correlation at finite temperatures. As seen in Figs. 3(b) and 3(c), for weaker coupling to the leads, the valley conductance quenches and the detector dips reduce, simultaneously. For strongly pinched off QD the detector dips disappear [11]. Similar correspondence is seen in Fig. 4 as the temperature increases. Both QD conductance and detector's sharp dips quench approximately on the scale of T_K (about 1 K is our device). Note that although application of V_{DS} quenches the valley conductance, Kondo correlation with the leads persists. Indeed, the dips do not vanish at finite V_{DS}; moreover, they split to doublets (not shown here).

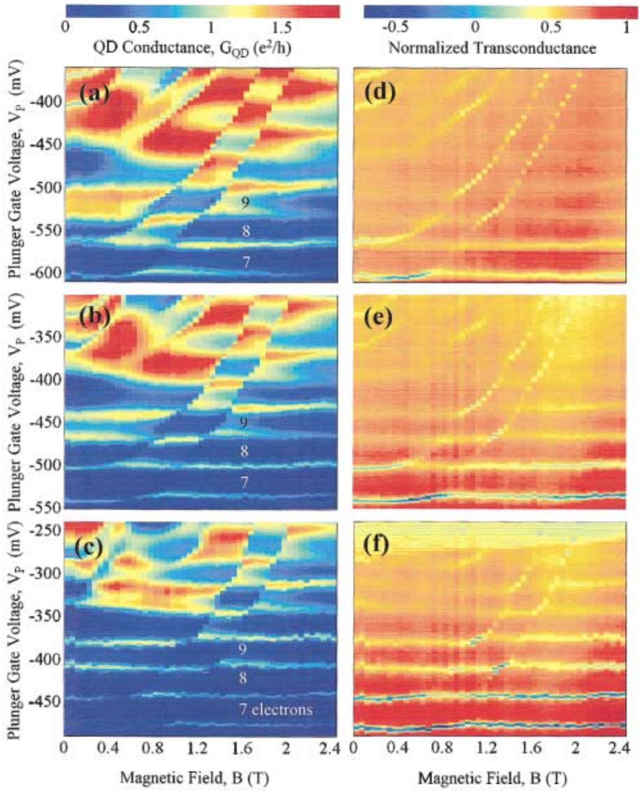

FIG. 3 (color). The 2D color plots of the conductance through the QD [left plots (a)–(c)] and the detector signal [right plots (d)–(f)] as a function of V_P and B perpendicular to the device. Top: strongest coupling to the leads. Bottom: weakest coupling to the leads. The three different coupling strengths are obtained by changing the two gate voltages, V_{g1} and V_{g2} (more negative bias for weaker coupling) and compensating by the bias on V_P so the QD is in the same electronic configuration. The voltage on the QPC detector is also tuned to keep its conductance at about e^2/h. The number of electrons is marked for some CB valleys. The detector signal in each plot is normalized by the maximum value of each plot since the detector signal sensitivity depends on the QD configuration.

The peculiar coincidence between abrupt charge reconfiguration and the onset of Kondo correlation can be related to level crossing in the QD. As B and V_P vary, quantum states cross each other and charge transfers to the lower energy state, leading to charge redistribution and to spin reconfiguration. We propose a model [12], depicted in Fig. 5, based, in principle, on the energy level spectrum of a 2D parabolic well with an applied magnetic field [13]. We assume that some states, localized to the center of the QD (weakly coupled to the leads), have strong magnetic field dependence [14]. Consequently, with increasing magnetic field these states cross other, more extended, states (better coupled to the leads), which have weaker magnetic field dependence. This can lead to charge reconfiguration accompanied by the onset of Kondo correlation. We neglect Zeeman splitting in our model since it quenches the Kondo effect only at higher magnetic field (above 2–3 T) [3].

We now apply these assumptions to our experimental results to see how the model works. The 2D plot in Fig. 3

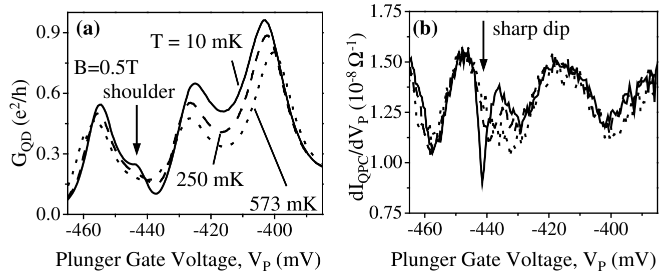

FIG. 4. Temperature dependence of the QD conductance in (a) and the sharp dip in the detector signal in (b). The measurement is performed at $B = 0.5$ T so that the sharp dip appears approximately in the middle of a CB valley. The visible shoulder in the conductance forms because a transition from a Kondo regime (left of the shoulder) to a non-Kondo regime (right of the shoulder) occurs at this point.

is first schematically reproduced in Fig. 5(a); K and NK stand for the Kondo and non-Kondo regimes, respectively. At $V_P = V_{P1}$ and $B = 0$ the QD is spin polarized with seven electrons; however, it is in a NK regime. Therefore, the seventh electron must occupy a localized state. The single particle spectrum that corresponds to this case is shown in Fig. 5(b). As the magnetic field increases, the energy of the localized state increases, finally crossing at $B = B_1$ the extended state. The seventh electron, seeking the lowest energy, hops to the extended state, and a sharp dip appears in the detector's signal while Kondo correlation forms [15]. Increasing V_P to V_{P2} [still keeping seven electrons in the QD, Fig. 5(a)] shifts the whole spectrum, but the localized state shifts faster than the extended states [16]. Thus the crossover energy of localized and extended states moves to a higher field $B = B_2$ [in Fig. 5(a)]. This reproduces the 2D path of the sharp dip for seven electrons in the QD.

Increasing the plunger gate voltage further to $V_P = V_{P3}$ [Fig. 5(a)], overcoming the charging energy, increases the number of electrons in the QD to eight. At $B = 0$ the last two electrons occupy the same localized state with net spin zero. As the magnetic field increases, the localized state approaches an extended state, and at $B = B_3$ in Fig. 5(c) it becomes energetically favorable for one electron to flip its spin and hop to the extended state (actually, in the two electron spectrum, this state is the ground state [17]). The total energy is then minimized since electron-electron interaction is reduced. This process is similar to a singlet-to-triplet transition already observed in QDs [18] and is similar to the recent observation of the Kondo effect in the unitary limit [19]. The transition reconfigures the charge and polarizes the QD enabling the Kondo correlation to take place. At $B = B_4$ level crossing takes place, and it becomes energetically favorable for the last two electrons to occupy the extended state with net spin zero in the QD (assuming weak e-e interaction in this state). Consequently, the charge reorganizes again, and Kondo correlation ceases. Similar arguments apply for $V_P = V_{P4}$ with nine electrons in the QD, and the ninth electron is in an extended state at $B = 0$ [K regime in Figs. 5(a) and 5(d)].

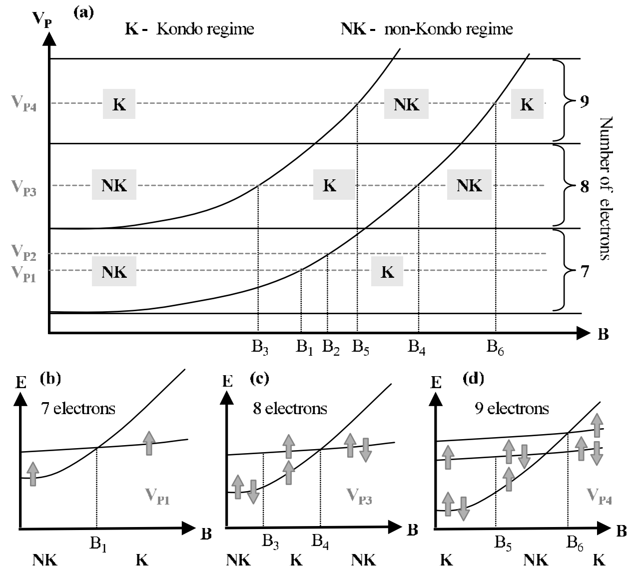

FIG. 5. (a) A 2D plot of $B - V_P$ reconstructing the bottom half of the top plots in Fig. 3. Horizontal solid lines correspond to CB peaks. Curved solid lines correspond to the charge reconfiguration lines (i.e., sharp dips in the detector). Crossing of sets of lines forms a chessboard pattern. (b), (c), and (d) are a suggested spectrum of levels as a function of magnetic field, corresponding to V_{P1}, V_{P3}, and V_{P4}, respectively.

This model explains the main features of our experiment and the correlation between the onset of the Kondo effect and charge redistribution. It is not clear why detector dips disappear when Kondo correlation is being quenched, since level crossing and charge redistribution still take place in the CB regime. This may be due to the smaller difference between the capacitance of the localized and the extended states in such QDs. Alternatively, the correlation between the appearance of charge reconfiguration in the QD and the onset of the Kondo effect may suggest *spin-charge correlation*—as the electron moves from a localized to an extended state (or back). Nevertheless, in the absence of a magnetic field, we show clear spin-charge separation in the Kondo correlated regime, and the charge is unaffected by the onset of Kondo correlation.

We thank Y. Oreg, Y. Meir, A. Silva, and S. Levit for many fruitful discussions. The work was partly supported by the MINERVA Foundation and the German Israeli Project Cooperation (DIP).

[1] J. Kondo, in *Solid State Physics,* edited by H. Ehrenreicht, F. Seitz, and D. Turnbull (Academic Press, New York, 1969), Vol. 23, p. 183; P.W. Anderson, Phys. Rev. **124**, 41 (1961).

[2] L. I. Glazman and M. E. Raikh, JETP Lett. **47,** 452 (1988); T. K. Ng and P. A. Lee, Phys. Rev. Lett. **61**, 1768 (1988).

[3] D. Goldhaber-Gordon *et al.,* Nature (London) **391**, 156 (1998).

[4] U. Meirav and E. B. Foxman, Semicond. Sci. Technol. **11**, 255 (1996).

[5] M. Field *et al.,* Phys. Rev. Lett. **70**, 1311 (1993); E. Buks *et al.,* Nature (London) **391**, 871 (1998); D. Berman *et al.,* Phys. Rev. Lett. **82**, 161 (1999).

[6] Y. Meir, N. S. Wingreen, and P. A. Lee, Phys. Rev. Lett. **70**, 2601 (1993); N. S. Wingreen and Y. Meir, Phys. Rev. B **49**, 11 040 (1994).

[7] Correction to the average charge is expected to be negligibly small [Y. Meir (private communication)].

[8] J. Schmid *et al.,* Phys. Rev. Lett. **84**, 5824 (2000).

[9] M. Keller *et al.,* Phys. Rev. B **64**, 033302 (2001).

[10] Since charge is not exactly an integer due to charge fluctuation to the leads, there could still be some small change in the total average charge [Y. Meir and N. S. Wingreen (private communication)].

[11] When the QD configuration is changed, the mutual capacitance between the QD and the detector changes slightly; however, this change is estimated to be too small to affect the measurement.

[12] Y. Oreg, Y. Meir, and N. S. Wingreen (private communication).

[13] C. G. Darwin, Proc. Cambridge Philos. Soc. Math. Phys. Sci. **27**, 86 (1930); V. Fock, Z. Phys. **47**, 446 (1928).

[14] In Darwin-Fock spectrum [13] for a few electrons in the QD, states that are more localized tend to rise faster with *B* than states that are more extended [schematically shown in Fig. 5(b)].

[15] This can be ascribed to the fact that the capacitance is different between localized and extended states. The jump in the QD potential is evident from the formula $\phi_{QD} = V_P \frac{C_{P\text{-}QD}}{C_{QD}}$, where $C_{P\text{-}QD}$ is the capacitance between the plunger gate and QD.

[16] The rate at which a level shifts with V_P depends on the QD capacitance (Ref. [15]).

[17] S. Tarucha *et al.,* Phys. Rev. Lett. **84**, 2485 (2000).

[18] L. P. Kouwenhoven *et al.,* Science **278**, 1788 (1997).

[19] W.G. van der Wiel *et al.,* Science **289**, 2105 (2000); J. Nygard, D. H. Cobden, and P. E. Lindelof, Nature (London) **408**, 342 (2000).